Acta Crystallographica Section B
Structural Science
ISSN 0108-7681

New monocyclic and acyclic hNK-2 antagonists retaining the β-turn feature. X-ray and molecular modelling studies

Maria Altamura,[a] Paolo Dapporto,[b]* Valentina Fedi,[a] Alessandro Giolitti,[a] Annalisa Guerri,[b] Antonio Guidi,[a] Carlo Alberto Maggi,[a] Paola Paoli[b] and Patrizia Rossi[b]

[a]Menarini Ricerche SpA, Via dei Sette Santi 3, 50131 Florence, Italy, and [b]Department of Energy Engineering 'S. Stecco', University of Florence, Via di S. Marta 3, 50139 Florence, Italy

Correspondence e-mail: paolo.dapporto@unifi.it

Received 28 February 2006
Accepted 16 May 2006

The human tachykinin NK-2 (hNK-2) receptor is considered a promising target for relevant pathologies at the respiratory, gastrointestinal and genitourinary level. With the aim of reducing the complexity of existing peptide antagonists, two series of hNK-2 receptor antagonists were designed, with the support of modelling, and synthesized. The X-ray structure determination of two compounds, each belonging to one of the two series, allowed the experimental validation of the initial rationale. In addition, it has been found that the two series share a β-turn structure, a key feature for binding the hNK-2 receptor.

1. Introduction

The tachykinin NK-2 receptor, a G protein-coupled membrane receptor, is mainly activated by Neurokinin A, one of the peptides of the tachykinin family. The human tachykinin NK-2 (hNK-2) receptor is considered a promising target for relevant pathologies at the respiratory, gastrointestinal and genitourinary level, where this receptor is mainly localized (Maggi *et al.*, 1993; Lecci *et al.*, 2004). Several peptidic and non-peptidic antagonists to this receptor are known, and a few of them are progressing to clinical studies (Lordal *et al.*, 2001; Fattori *et al.*, 2004; Quartara & Altamura, 2006). One of the most potent antagonists for the tachykinin NK-2 receptor is the bicyclic peptide MEN10627 [cyclo(-Met^1-Asp^2-Trp^3-Phe^4-Dap^5-Leu^6-)cyclo(2β-5β); Dap = 2,3-diaminopropionic acid] (Pavone *et al.*, 1995). Its very low bioavailability, however, prevents it from being used as a drug. We have already shown (Giannotti *et al.*, 2000; Giolitti *et al.*, 2002) the design rationale for reducing its size and complexity, selecting part of the structure retaining the β-turn feature of one of the cycles, which we considered responsible for the ability to effectively bind the hNK-2 receptor. Two series of hNK-2 antagonists originated deriving from theoretical assumptions with the support of modelling: a monocyclic one (Fedi *et al.*, 2004) and a further simplified linear one (Sisto *et al.*, 2003). The latter was developed to circumvent the low oral bioavailability which still was limiting the use of the monocyclic compounds. Antagonists from this latter series are presently undergoing preclinical development. In the present work we show how subsequently that rationale was experimentally validated, through X-ray structural determination of *N*-[5(*S*),8(*R*)-dibenzyl-2(*S*)-(1*H*-indol-3-ylmethyl)-3,6,11,14-tetraoxo-1,4,7,-10-tetraazacyclotetradec-12(*R*)-yl]-2-(4-sulfamoylpiperazin-1-yl)acetamide [MEN13365, (1)] and 6-methylbenzo[*b*]thio-]thiophene-2-carboxylic acid [1-(2-phenyl-1*R*-{[1-(tetrahydropyran-4-ylmethyl)piperidin-4-ylmethyl]carbamoyl}ethylcarba-

Table 1
Experimental table.

	(1)·3C_2H_5OH·H_2O	(2)
Crystal data		
Chemical formula	$C_{45}H_{67}N_9O_{11}S$	$C_{37}H_{48}N_4O_4S$
M_r	942.14	644.85
Cell setting, space group	Orthorhombic, $P2_12_12_1$	Monoclinic, $P2_1$
Temperature (K)	298	298
a, *b*, *c* (Å)	11.359 (3), 18.383 (4), 23.325 (7)	14.0346 (8), 9.8834 (7), 25.617 (2)
α, β, γ (°)	90.00, 90.00, 90.00	90.00, 98.152 (3), 90.00
V (Å^3)	4871 (2)	3517.4 (4)
Z	4	4
D_x (Mg m^{-3})	1.285	1.218
Radiation type	Cu $K\alpha$	Cu $K\alpha$
μ (mm^{-1})	1.15	1.16
Crystal form, colour	Prism, colourless	Parallelepipedon, pale yellow
Crystal size (mm)	0.6 × 0.4 × 0.3	0.4 × 0.4 × 0.3
Data collection		
Diffractometer	Three-circle SMART CCD	Three-circle SMART CCD
Data collection method	Intensity from ω scans	Intensity from ω scans
Absorption correction	Empirical (using intensity measurements)	Empirical (using intensity measurements)
T_{min}	0.564	0.665
T_{max}	0.705	0.705
No. of measured, independent and observed reflections	8834, 5411, 4612	13 267, 7090, 5160
Criterion for observed reflections	$I > 2\sigma(I)$	$I > 2\sigma(I)$
R_{int}	0.037	0.043
θ_{max} (°)	56.5	57.1
Refinement		
Refinement on	F^2	F^2
$R[F^2 > 2\sigma(F^2)]$, $wR(F^2)$, S	0.052, 0.138, 1.03	0.075, 0.187, 1.07
No. of reflections	5411	7090
No. of parameters	597	831
H-atom treatment	Constrained to parent site	Constrained to parent site
Weighting scheme	$w = 1/[\sigma^2(F_o^2) + (0.0854P)^2 + 0.3813P]$, where $P = (F_o^2 + 2F_c^2)/3$	$w = 1/[\sigma^2(F_o^2) + (0.1097P)^2]$, where $P = (F_o^2 + 2F_c^2)/3$
$(\Delta/\sigma)_{max}$	<0.0001	<0.0001
$\Delta\rho_{max}$, $\Delta\rho_{min}$ (e Å^{-3})	0.54, −0.35	0.26, −0.18
Absolute structure	Flack (1983)	Flack (1983)
Flack parameter	0.03 (3)	0.08 (4)

Computer programs used: *SMART*, *SAINT*, *SIR*97 (Altomare *et al.*, 1999), *SHELXL*97 (Sheldrick, 1997), *ORTEP*3 (Farrugia, 1997), *PARST*97 (Nardelli, 1995).

moyl)cyclopentyl]amide [MEN15596, (2)] belonging respectively to the first and the second of the above-mentioned series. We also show how the features we have noticed in the first series of antagonists have been retained in the new linear compounds.

2. Experimental and computational methods

Suitable crystals of (1) were obtained by crystallization in sequence from absolute ethanol and acetone. (1) was initially dissolved in hot ethanol and the solution allowed to stand for one night at room temperature (r.t.). The crystals obtained were collected by filtration, dissolved again in hot acetone and the solution was allowed to stand for 48 h, then filtered obtaining crystals of (1) suitable for X-ray analysis (m.p. 526–527 K). In order to obtain suitable crystals, (2) was dissolved in hot ethyl acetate and the solution allowed to cool to room temperature; some drops of petroleum ether 40–60° were then added. After standing at room temperature for 2 d, crystals were filtered off and dissolved again in hot ethyl acetate and the solution was allowed to stand at room temperature in a chamber saturated with vapour of petroleum ether 40–60° for 1 week. The crystals obtained of (2) were suitable for X-ray analysis (m.p. 468–469 K). Data collection and refinement parameters are summarized in Table 1. Diffraction studies were carried out with a Siemens/Bruker diffractometer equipped with a rotating anode and SMART 1K CCD area detector. Data collections were carried out using the program *SMART* (Siemens, 1995). Five sets of data were pulled together using the narrow frames method with a 0.3° increment in ω. A total of 3000 frames were collected. Data reductions were carried out using the program *SAINT* (Siemens, 1995). Absorption corrections were applied through the program *SADABS* (Sheldrick, 1996). In both structures all the non-H atoms were refined anisotropically and the H atoms were all set in calculated positions and refined isotropically. The absolute configurations were assigned on the basis of the Flack parameter [x = 0.03 (3) for (1) and x = 0.08 (4) for (2); Flack, 1983]. Crystallographic data have been deposited.[1]

Conformational analyses were performed with a simulated annealing protocol in *Sybyl*6.4 (Tripos, USA). Mean distances were calculated, using the lower-energy conformers, between centroids on the ring systems and the charged amino group [in the piperazine ring in (1), and in the piperidine ring in (2)]. The pharmacophore model referred to in this work was obtained by comparing the relative position in space of the common features in a larger series of compounds. The superimposition of the above-mentioned features among all the low-energy conformers considered defined the pharmacophore points.

3. Results and discussion

3.1. X-ray structure analyses

3.1.1. (1)·3C_2H_5OH·H_2O. In the asymmetric unit there is an independent molecule of (1) (see Fig. 1*a*), three molecules of ethanol and a water molecule.

All the peptide bonds of (1) have a *trans* conformation. The C_α atoms of the D-Asp[1]-Trp[2]-Phe[3] segment as well as the α-C atom of Dia[4] [Dia: (2*R*)-1,2-diamino-2-benzylethane] occupy

[1] Supplementary data for this paper are also available from the IUCr electronic archives (Reference: GP5007). Services for accessing these data are described at the back of the journal.

the corners of the rectangle outlined by the backbone atoms (Fig. 2).

Given the 14-membered cycle, the benzyl moiety of Phe^3 is positioned on the opposite side with respect to the amino-sulfonyl piperazine pendant bound to D-Asp^1 as well as to the side-chains of Trp^2 and Dia^4 (Fig. 3).

The aromatic rings of Trp^2 and Phe^3 point away from the cycle peptide cavity. However, while the phenyl ring of Phe^3 is almost parallel to it, as shown by the angle [18.1 (1)°] between the aromatic ring and the mean plane described by the 14-membered ring, this latter forms an angle of 68.52 (7)° with the plane of the two condensed cycles of Trp^2. On the contrary, the side-chain on D-Asp^1 and the benzyl moiety of Dia^4 are almost perpendicular to the peptide cavity. The Trp^2-Phe^3 peptide segment shows φ and ψ dihedral angles typical of those of positions 2 and 3 of a type-I β-turn (Sibanda *et al.*, 1989; Kabsch & Sander, 1983; see Table 2).

This conformation is stabilized by an intra-turn hydrogen bond between the C′O group of D-Asp^1 and the NH group of Dia^4 (Fig. 2, Table 3). Concerning the side-chain on D-Asp^1, the hydrogen-bond donor nature of the aspartate NH group (Table 3) stabilizes the observed conformation.

The Trp^2 and Phe^3 side-chains adopt the typical *gauche*(+) conformation in which the γ side-chain atom is opposite the main chain carbonyl group of the residue (Table 2). Also their χ^2 angles take the values (*ca.* $\pm 90°$) usually expected for residues with an sp^2 hybridized γ atom in order to minimize close contacts. The benzyl moiety of Dia^4 shows the less common *gauche*(−) conformation about χ^1, while χ^2 have the expected values. The side-chain attached on C_α of D-Asp^1 has a *trans–cis* arrangement about N5—C11 and C11—C12, respectively.

The similarity in the backbone as well as in the residue sequences between (1) and part of MEN10627 (Pavone *et al.*, 1995) prompted us to compare the three-dimensional arrangement of the two molecules. The C atoms residing at the corners of the 14-membered ring of (1) were superimposed with respect to those occupying the analogous positions in MEN10627 so that the Trp-Phe sequence is almost coincident for both the molecules. The resulting drawing (Fig. 4) highlights the unsurprisingly three-dimensional similarity of the backbone defining the peptide rings given that both feature a type-I β-turn as well as an intra-turn hydrogen bond stabilizing the reversal of the chain.

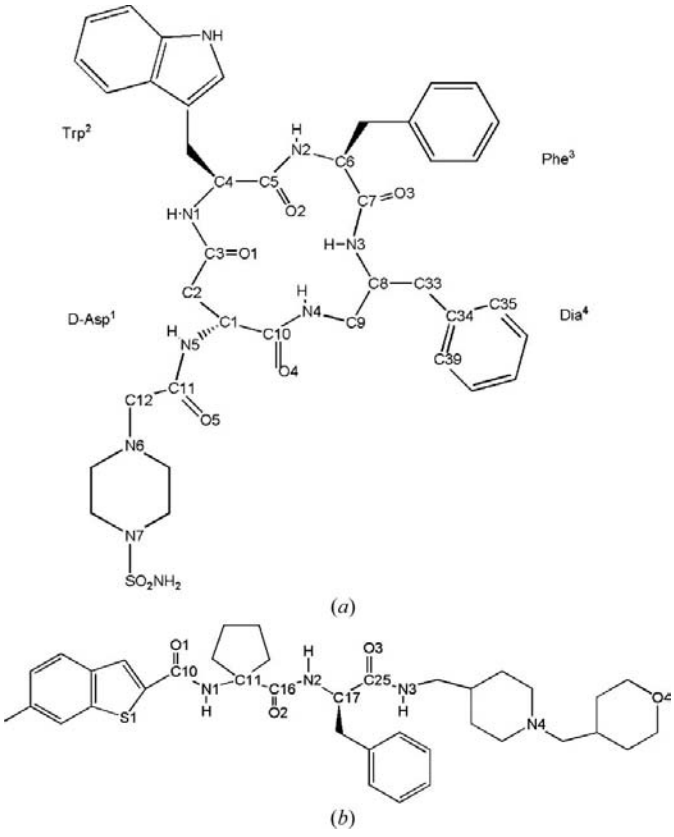

Figure 1
Schematic drawings of (*a*) (1) and (*b*) (2) with essential labelling scheme.

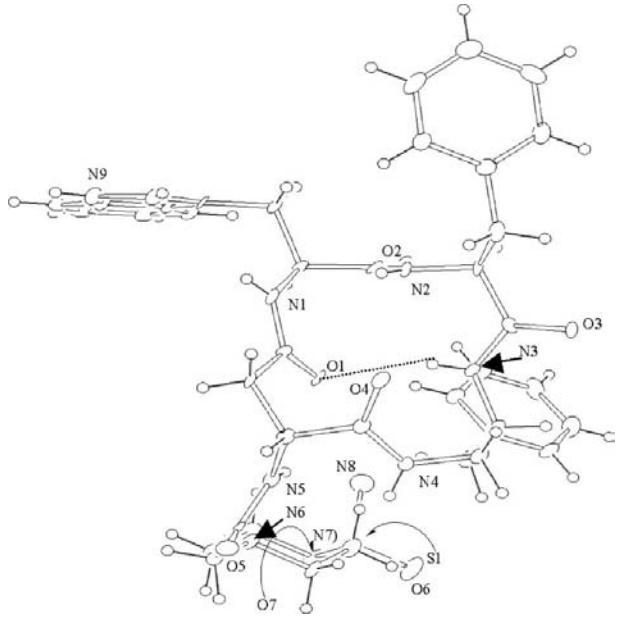

Figure 2
*ORTEP*3 top view of (1). Displacement ellipsoids are drawn at 30% probability.

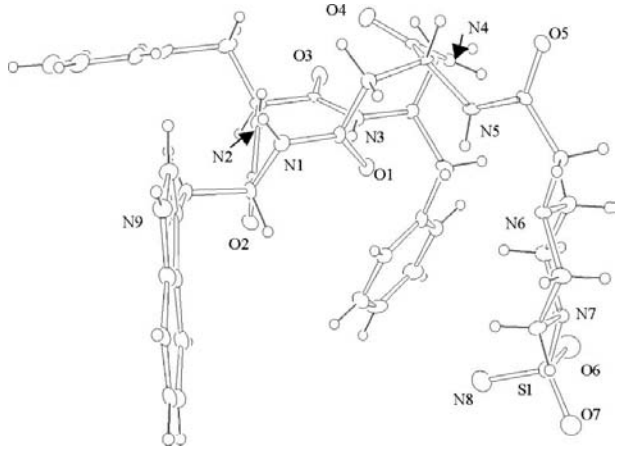

Figure 3
*ORTEP*3 side view of (1). Displacement ellipsoids are drawn at 30% probability.

Table 2
Most important torsional angles defining the molecular shape of (1) as derived from the X-ray structure (°, estimated standard deviations in parentheses, see Fig. 1 for atom labelling).

	D-Asp[1]	Trp[2]	Phe[3]	Dia[4]
φ	118.81 (4)	−60.7 (5)	−95.4 (5)	
ψ	−16.5 (6)	−30.0 (6)	11.4 (6)	
ω	171.0 (4)	−176.0 (4)	−177.2 (4)	
χ^1	−71.9 (4)	−62.5 (5)	−73.6 (5)	63.7 (5)†
$\chi^{2,1}$	−159.6 (4)‡	95.3 (6)	79.0 (6)	−92.9 (5)§
$\chi^{2,2}$	21.0 (6)¶	−81.1 (6)	−100.7 (5)	84.5 (5)††
N4—C10—C1—C2	−141.2 (4)			
C10—C1—C2—C3	54.5 (5)			
N3—C8—C9—N4				67.6 (5)
C7—N3—C8—C9				93.7 (5)

† N3—C8—C33—C34. ‡ C1—C2—C3—N1. § C8—C33—C34—C35. ¶ C1—C2—C3—O1. †† C8—C33—C34—C39.

On the contrary, they differ in the orientation of the Phe side-arm (Δx^1 and Δx^2 about 40°) and in the orientation about χ^2 of the Trp residue. Finally, the conformation of the side-chain on D-Asp[1] is almost superimposable, at least up to the dihedral about C11—C12 to the backbone of the condensed peptide cycle of MEN10627. As also expected, the X-ray structure of the pseudo-symmetrical analogue cycle (Phe[1]-Asp[2]-Trp[3]-Phe[4]-Dap[5]-Trp[6])cycle(2β-5β) (MEN10698; Lombardi *et al.*, 1997) shows a very similar arrangement of the backbone atoms with respect to (1), since both its independent molecules display a type-I β-turn featuring the Trp[3]-Phe[4] peptide segment (Fig. 5).

The conformation of the pendant arms of the latter fragment in MEN10698 as defined by χ^1 compares well with those equivalent to (1), while the χ^2 dihedral angles, especially those concerning Trp[2] [in (1)] and Trp[3] in the pseudo-symmetrical parent peptide, show the most significant differences.

Table 3
Intramolecular hydrogen bonds in (1) as obtained from X-ray analysis.

Donor···Acceptor	Distance (Å) Donor···Acceptor	Angle (°) Donor—H···Acceptor
N3···O1	3.170 (5)	159.0 (3)
N5···O1	2.887 (5)	115.8 (3)
N5···N6	2.704 (5)	109.8 (2)

Concerning the crystal packing, each molecule of (1) interacts *via* hydrogen bonds with four identical symmetry-related molecules: the NH and γNH groups of Trp[2] and Dia[4] are hydrogen-bond donors to an O atom of the aminosulfonyl moiety [N1···O7^{i}, 2.966 (5) Å, (i) $-x+\frac{1}{2}+1, -y, z-\frac{1}{2}$] and to that of Phe[3] CO [N4···O3^{ii}, 3.047 (5) Å, (ii) $x-\frac{1}{2}, -y+\frac{1}{2}, -z$], respectively, and obviously the converse holds. The O atom of a crystallization water molecule is a hydrogen-bond donor to D-Asp[1]CO [O8···O4, 2.801 (5) Å], while a symmetry-related image of it interacts with atom N8 of the SO_2NH_2 group [O8^{iii}···N8, 2.805 (6) Å, (iii) $-x+\frac{1}{2}+1, -y, z+\frac{1}{2}$]. At the same time the indolyl Trp[2]εNH is a hydrogen-bond donor to the O atom of a molecule of ethanol [N9···O9, 2.838 (6) Å] and a symmetry image of the latter works as a donor to Trp[2] CO [O9^{iv}···O2, 2.744 (4) Å, (iv) $x+\frac{1}{2}, -y-\frac{1}{2}, -z$]. Finally, several close contacts exist between the water molecule and the remaining crystallization ethanol molecules.

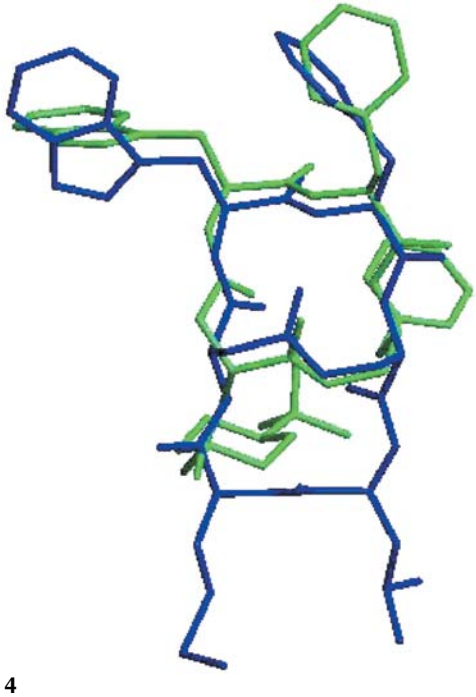

Figure 4
Superimposition of (1) (green) and MEN10627 (blue).

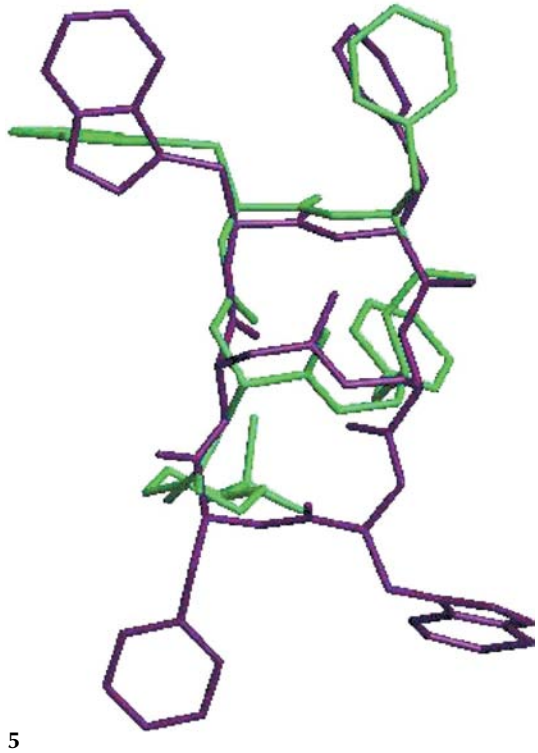

Figure 5
Superimposition of (1) (green) and MEN10698 (purple). Only one independent molecule of the latter species was considered for comparative purposes, given that the two independent molecules have a very similar conformation.

Table 4
Most important torsion angles defining the molecular shape in (2) as derived from the X-ray structure (°; see Fig. 1 for atom labelling).

	a†	*b*‡
φ(Cyc^2)	66 (1)	−60.8 (9)
φ(D-Phe^3)	104.4 (8)	−73.7 (9)
ψ(Cyc^2)	30 (1)	−35.6 (9)
ψ(D-Phe^3)	29 (1)	−10 (1)
ω(Cyc^2)	166.5 (7)	−174.6 (6)
ω(D-Phe^3)	174.2 (7)	179.9 (7)
χ^1(D-Phe^3)	63.1 (8)	56.2 (9)
$\chi^{2,1}$(D-Phe^3)	14 (1)	81 (1)
$\chi^{2,2}$(D-Phe^3)	−165.8 (8)	−103 (1)

† Isomer *a*: φ_{Cyc} = C10*a*—N1*a*—C11*a*—C16*a*, ψ_{Cyc} = N1*a*—C11*a*—C16*a*—N2*a*, $\varphi_{D\text{-}Phe}$ = C16*a*—N2*a*—C17*a*—C25*a*, $\psi_{D\text{-}Phe}$ = N2*a*—C17*a*—C25*a*—N3*a*. ‡ Isomer *b*: φ_{Cyc} = C10*b*—N1*b*—C11*b*—C16*b*, ψ_{Cyc} = N1*b*—C11*b*—C16*b*—N2*b*, $\varphi_{D\text{-}Phe}$ = C16*b*—N2*b*—C17*b*—C25*b*, $\psi_{D\text{-}Phe}$ = N2*b*—C17*b*—C25*b*—N3*b*.

3.1.2. (2). The asymmetric unit of (2) (see Fig. 1*b*) contains two independent molecules (*a* and *b* in Fig. 6).

The two molecules mainly differ in the conformation of the backbone atoms, especially the region featuring the piperidine-tetrahydropyran groups. Adopting the usual classification for peptide structures, the C atoms of the backbone describe a β-turn involving the 1-aminocyclopentanecarboxylic acid (considered as the amino acid in the second position, Cyc^2 hereafter) and the D-phenylalanine (in the third position, D-Phe^3) residues. The corresponding dihedral angles defining the β-turn motif are reported in Table 4.

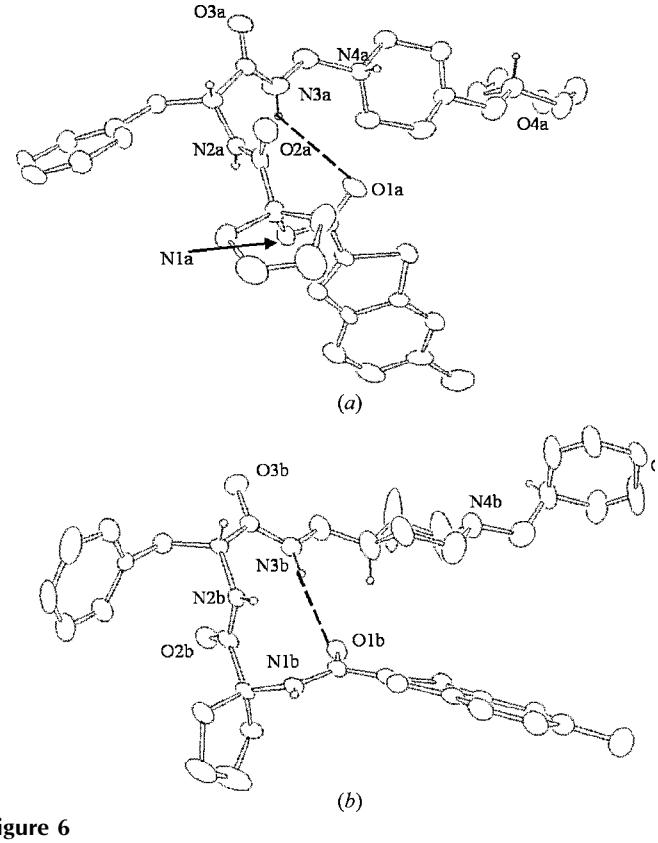

Figure 6
*ORTEP*3 views of the two independent molecules of (2). Displacement ellipsoids are drawn at 30% probability.

Table 5
Hydrogen bonds involved in the β-turn in (2) as obtained from X-ray analysis.

Isomer	Donor···Acceptor	Distance (Å) Donor···Acceptor	Angle (°) Donor—H···Acceptor
a	N3*a*···O1*a*	3.803 (9)	132.1 (5)
b	N3*b*···O1*b*	3.136 (8)	163.8 (4)

For molecule *a* in particular, a type-I′ β-turn (Hutchinson & Thornton, 1994; Vidya Harini *et al.*, 2005) can be identified, while a type-I β-turn is present in *b*. The different β-turn type could account for the RMS value (0.98 Å) resulting from the superimposition (shown in Fig. 7) of the backbone atoms of the two conformational isomers.

In both cases the β-turn causes the formation of two chain reversals, causing each molecule to bend over itself. This structuring effect is to be attributed to the α,α-disubstituted amino acid (1-aminocyclopentanecarboxylic acid). As usual, the reverse turn is stabilized in both the conformational isomers by a hydrogen bond between the carbonylic O atom of residue 1, containing the benzothiophene moiety, and the amide H atom of the residue in the fourth position including the piperidine ring (Table 5). In *a* this interaction is weak [N3*a*···O1*a* 3.803 (9) Å], while in *b* the hydrogen bond is stronger as shown by the shorter N3*b*···O1*b* distance [3.136 (8) Å].

Regarding the side chain, the orientation of the phenylalanine residue in the two molecules is quite different: while χ^1 angles have comparable values [63.1 (1)° *versus* 56.2 (9)° in *a* and *b*, respectively], χ^2 is definitively different (Table 4). As a consequence, the phenyl ring points in different directions in the two fragments. In both *a* and *b* the saturated rings show their usual conformations.

In the crystal lattice, intermolecular interactions of different nature can be recognised, *i.e.* hydrogen bonds and interactions concerning hydrophobic groups such as the aromatic ones.

Each independent molecule (*a* and *b*) interacts *via* hydrogen bonds with four molecules of (2): two of them are of the *a* isomer and the others are of type *b*. The whole pattern of hydrogen-bond interactions is reported in Fig. 8, while Table 6 sums up the bond distances and angles.

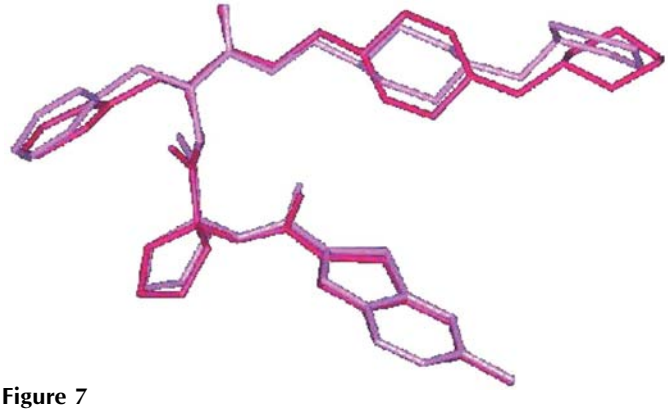

Figure 7
Superimposition of the two independent molecules *a* (dark pink) and *b* (light pink) of (2).

Table 6
Intermolecular hydrogen bonds in the crystal lattice of (2) as obtained from X-ray analysis.

Donor···Acceptor	Distance (Å) Donor···Acceptor	Angle (°) Donor—H···Acceptor
N1*a*···O4*b*	3.00 (1)	147.1 (5)
N2*a*···O3*a*	3.028 (8)	156.5 (4)
N3*a*···O3*a*	3.24 (1)	143.6 (5)
N1*b*···O4*a*	3.100 (9)	164.5 (5)
N2*b*···O3*b*	2.928 (8)	160.7 (4)

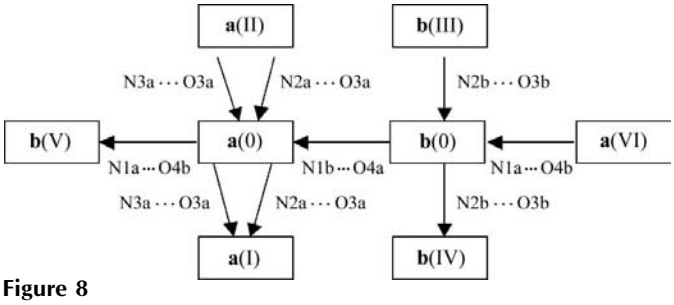

Figure 8
Hydrogen-bond interactions of isomers *a* and *b* of (2). Molecules are reported by the following symmetry operations: (I) $-x+1, y-\frac{1}{2}, -z+2$; (II) $-x+1, y+\frac{1}{2}, -z+2$; (III) $-x, y-\frac{1}{2}, -z+1$; (IV) $-x, y+\frac{1}{2}, -z+1$; (V) $x+1, y, z+1$; (VI) $x-1, y, z-1$.

Taking as reference molecules *a*(0) and *b*(0) in Fig. 8, these are held together by a hydrogen bond between O4*a* of *a* and N1*b* of *b*, the latter acting as a donor. Concerning molecule *a*(0), N1*a*, N2*a* and N3*a* are hydrogen-bond donors to carbonyl O atoms. In particular, N1*a* interacts with O4*b* of *b*(V) and N2*a* and N3*a* with O3*a* of a symmetry-related molecule *a*(I). Obviously the same atom O3*a* in *a*(0) works as an acceptor for the amide N2*a* and N3*a* atoms of *a*(II), and O4*b* in *b*(0) acts as a hydrogen-bond acceptor from N1*a* of *a*(VI). Atom O3*b* in *b*(0) is a hydrogen-bond acceptor from N2*b* of a symmetry image of *b*, namely *b*(III) in Fig. 8, and, correspondingly, *b*(0) is a hydrogen-bond donor, *via* N2*b*, to O3*b* of *b*(IV). It is worth noting that the equivalent carbonylic O2*a* and O2*b* atoms do not take part in any hydrogen-bond interactions, although they point outside the loop shaped by the backbone atoms and are not shielded by the closest hydrophobic groups.

Finally, several T-shaped intermolecular C—H···π interactions (Takahashi *et al.*, 2001) can be recognized. The benzothiophene moiety of both the conformational isomers *a* and *b* is involved as a π-electron donor, the positively charged H atoms being provided by both the cyclopentane as well as the phenyl ring. The C—H···π distances, evaluated by considering the centroid of the electron donor ring, range from 2.91 to 3.08 Å with the mean planes described by donor–acceptor rings almost perpendicular to each other. This is the common interaction between aromatic rings found in crystal structures, while in solution they are usually parallel (Gervasio *et al.*, 2000).

As a final remark, given that the architecture of the backbone of (1) is very similar to that of MEN10627 and MEN10698, the 14-membered cycle Asp[1]-Trp[2]-Phe[3]-Dia[4] also represents quite a rigid and preorganized simple peptide scaffold useful in the design of bioactive molecules featuring a type I β-turn motif. In this respect, isomer *b* of (2) could also play the same role, given its three-dimensional similarity with (1), as provided by the RMS value (0.12 Å) obtained by the superimposition of the backbone atoms in the β-turn of both the molecules (Fig. 9).

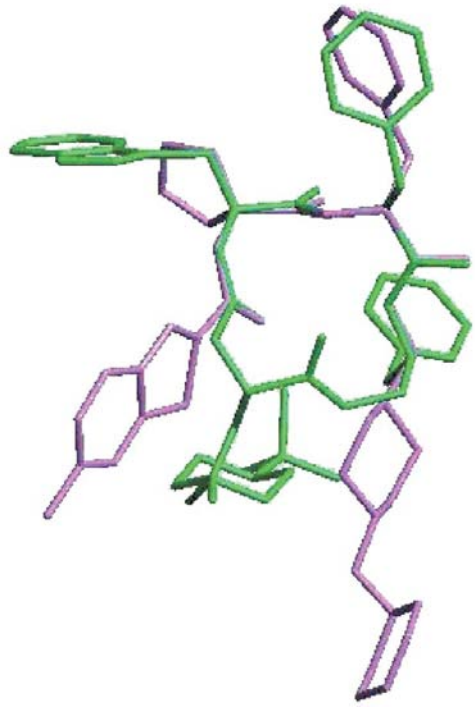

Figure 9
Superimposition of (1) (green) and the conformational isomer *b* of (2) (pink) featuring the type I β-turn.

3.2. Modelling studies

Previous to the crystal structure determinations, modelling studies were performed on both the monocyclic [*i.e.* (1)] and linear [*i.e.* (2)] compound series. A pharmacophore model (characterized by three hydrophobic and one positively charged groups) could be derived, whose features were previously defined with the help of point mutagenesis studies on a series of compounds belonging to this class (Giolitti *et al.*, 2000; Meini *et al.*, 2004). The energetic stability of the proper conformation has now been experimentally confirmed by the solid-state structures reported in this paper.

In fact, a remarkable geometrical correspondence (in terms of the relative distance separating the centroids of the groups, Table 7) was found between the three-dimensional arrangements of (1) and (2*b*) in the experimental structures and in the conformations derived from the modelling, albeit that the variability of the charged group position was quite large as can be expected from the flexibility of the carbon chains bearing those groups.

In (1) the hydrophobic centres are represented by the three aromatic rings of Trp[2], Phe[3] and Dia[4], while the positive charge is located on N6 (Fig. 10).

Table 7
Comparison of the distances (Å) defining the pharmacophore model of (1) and (2*b*) as derived by the X-ray structures and modelling studies.

X = geometrical centre of the ring system.

	Distances (Å)	
	X-ray structure	Modelling study
(1)		
$X(Trp^2)\cdots N$	8.66	9.00
$X(Phe^3)\cdots N$	11.55	11.00
$X(Dia^4)\cdots N$	6.73	6.70
$X(Trp^2)\cdots X(Dia^4)$	9.58	9.90
$X(Trp^2)\cdots X(Phe^3)$	8.26	7.10
$X(Dia^4)\cdots X(Phe^3)$	8.75	8.40
(2*b*)		
$X(Btp^1)\cdots N$	7.05	7.30
$X(Cyc^2)\cdots N$	9.31	9.40
$X(D\text{-}Phe^3)\cdots N$	11.30	10.60
$X(Btp^1)\cdots X(Cyc^2)$	6.67	6.60
$X(Btp^1)\cdots X(D\text{-}Phe^3)$	10.21	9.40
$X(Cyc^2)\cdots X(D\text{-}Phe^3)$	5.57	5.80

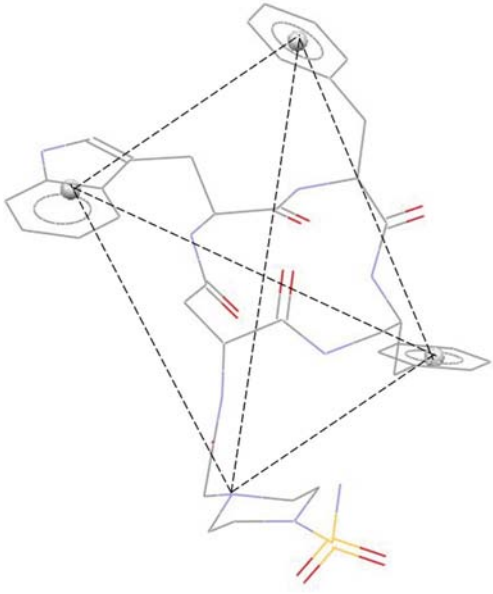

Figure 10
Pharmacophore model derived from the molecular modelling studies for (1). Spheres represent the centroids calculated using all the non-H atoms of the rings.

The benzothiophene system (Btp^1), together with the Cyc^2 and D-Phe^3 rings, characterize the hydrophobic part of the pharmacophore in (2) (Fig. 11). In this case the positively charged unit is the amino group of the piperidine.

4. Conclusion

The X-ray structures of (1) and (2) confirm our expectations of their molecular structure, particularly their ability to retain the β-turn, a key feature for binding the hNK-2 receptor. The molecular rigidity, owing to the presence of molecular residues having structuring effects, as the 1-aminocyclopentanecarboxylic acid in (2), is also confirmed by the satisfactory

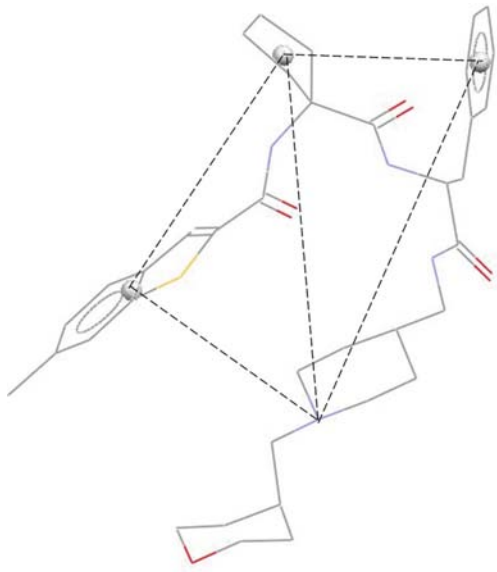

Figure 11
Pharmacophore model derived from the molecular modelling studies for (2). Spheres represent the centroids calculated using all the non-H atoms of the rings.

match between the pharmacophore models derived from the modelling studies and the solid-state structures for both the molecules.

CRIST (Centro Interdipartimentale di Cristallografia Strutturale), University of Florence, where the X-ray measurements were performed, is gratefully acknowledged. This work was supported in part by MIUR, Ministero dell'Istruzione, dell'Università e della Ricerca (Grant reference 4579/DSPAR/01).

References

Altomare, A., Cascarano, G. L., Giacovazzo, C., Guagliardi, A., Burla, M. C., Polidori, G., Camalli, M., Moliterni, A. G. & Spagna, R. (1999). *J. Appl. Cryst.* **32**, 115–121.
Farrugia, L. J. (1997). *J. Appl. Cryst.* **30**, 565.
Fattori, D., Altamura, M. & Maggi, C. A. (2004). *Mini-Rev. Med. Chem.* **4**, 331–340.
Fedi, V., Altamura, M., Balacco, G., Canfarini, F., Criscuoli, M., Giannotti, D., Giolitti, A., Giuliani, S., Guidi, A., Harmat, N. J. S., Nannicini, R., Pasqui, F., Patacchini, R., Perrotta, E., Tramontana, M., Triolo, A. & Maggi, C. A. (2004). *J. Med. Chem.* **47**, 6935–6947.
Flack, H. D. (1983). *Acta Cryst.* A**39**, 876–881.
Gervasio, F. L., Procacci, P., Cardini, G., Guarna, A., Giolitti, A. & Schettino, V. (2000). *J. Phys. Chem. B*, **104**, 1108–1114.
Giannotti, D., Perrotta, E., Di Bugno, C., Nannicini, R., Harmat, N. J. S., Giolitti, A., Patacchini, R., Renzetti, A., Rotondaro, L., Giuliani, S., Altamura, M. & Maggi, C. A. (2000). *J. Med. Chem.* **43**, 4041–4044.
Giolitti, A., Altamura, M., Bellucci, F., Giannotti, D., Meini, S., Patacchini, R., Rotondaro, L., Zappitelli, S. & Maggi, C. A (2002). *J. Med. Chem.* **45**, 3418–3429.
Giolitti, A., Cucchi, P., Renzetti, A. R., Rotondaro, L., Zappitelli, S. & Maggi, C. A. (2000). *Neuropharmacology*, **39**, 1422–1429.
Hutchinson, E. G. & Thornton, J. M. (1994). *Protein Sci.* **3**, 2207–2216.

Kabsch, W. & Sander, C. (1983). *Biopolymers*, **22**, 2577–2637.
Lecci, A., Capriati, A. & Maggi, C. A. (2004). *Br. J. Pharmacol.* **141**, 1249–1263.
Lombardi, A., D'Auria, G., Saviano, M., Maglio, O., Nastri, F., Quartara, L., Pedone, C. & Pavone, V. (1997). *Biopolymers*, **40**, 505–518.
Lordal, M., Navalesi, G., Theodorsson, E., Maggi, C. A. & Hellstrom, P. M. (2001). *Br. J. Pharmacol.* **34**, 215–223.
Maggi, C. A., Patacchini, R., Rovero, P. & Giachetti, A. (1993). *J. Auton. Pharmacol.* **13**, 23–93.
Meini, S., Bellucci, F., Catalani, C., Cucchi, P., Patacchini, R., Rotondaro, L., Altamura, M., Giuliani, S., Giolitti, A. & Maggi, C. A. (2004). *Eur. J. Pharmacol.* **488**, 61–69.
Nardelli, M. (1995). *J. Appl. Cryst.* **28**, 659.
Pavone, V., Lombardi, A., Nastri, F., Saviano, M., Maglio, O., D'Auria, G., Quartara, L., Maggi, C. A. & Pedone, C. (1995). *J. Chem. Soc. Perkin Trans. 2*, pp. 987–994.
Quartara, L. & Altamura, M. (2006). *Curr. Drug Targets.* In the press.
Sheldrick, G. M. (1996). *SADABS*. University of Göttingen, Germany.
Sheldrick, G. M. (1997). *SHELX*97. University of Göttingen, Germany.
Sibanda, B. L., Blundell, T. L. & Thornton, J. M. (1989). *J. Mol. Biol.* **206**, 759–777.
Siemens (1995). *SAINT*. Version 4.0. Siemens Industrial Automation, Madison, Wisconsin, USA.
Siemens (1995). *SMART*. Siemens Industrial Automation, Madison, Wisconsin, USA.
Sisto, A., Caciagli, V., Altamura, M., Giolitti, A., Fedi, V., Guidi, A., Giannotti, D., Harmat, N. J. S., Nannicini, R., Pasqui, F. & Maggi, C. A. (2003). International Patent Application WO 2003/37916; *Chem. Abstr.* **138**, 369197.
Takahashi, O., Kohno, Y., Iwasaki, S., Saito, K., Iwaoka, M., Tomoda, S., Umezawa, Y., Tsuboyama, S. & Nishio, M. (2001). *Bull. Chem. Soc. Jpn*, **74**, 2421–2430.
Vidya Harini, V., Aravinda, S., Rai, R., Shamala, N. & Balaram, P. (2005). *Chem. Eur. J.* **11**, 3609–3620.